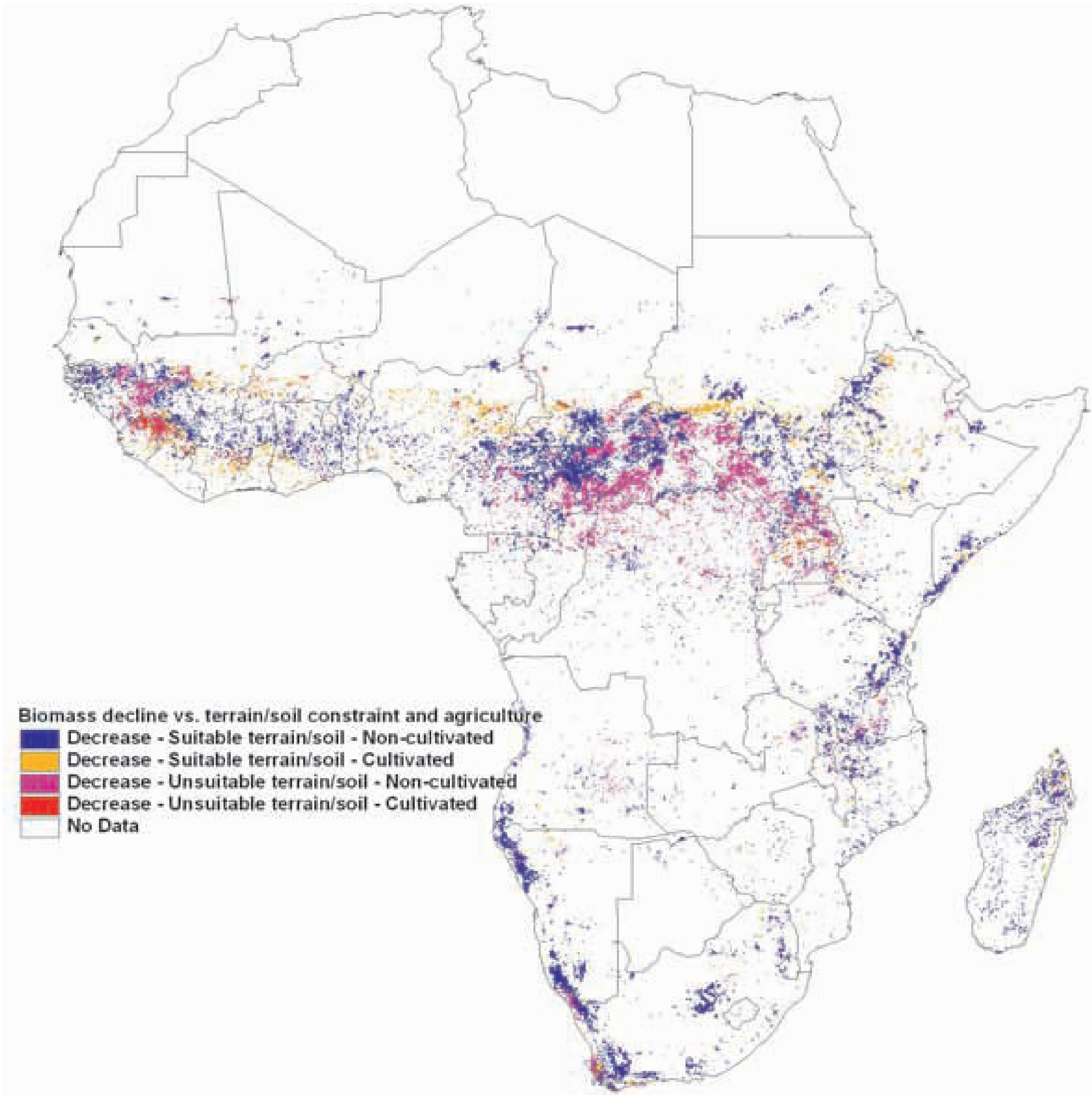

Map 11. Areas with biomass decline as function of soil/terrain constraints and their agricultural use. Note: (1) suitable soil/terrain includes good and bad soil/terrain conditions as in Maps 8a and 8b, and (2) cultivated land as from GLC2000 data (i.e., categories 3 and 6 in Map 10).

Table 10 Area of land-use/cover types calculated for each degradation class across soil/terrain constraints.

Degradation class	*Area of land-use/cover type (km²)*							*Total area (km²)*
	Dense forest	*Forest/ Savanna*	*Forest/ Cropland*	*Woodland/ Shrubland*	*Grassland*	*Agriculture*	*Others*	
Dry-Neutral/Negative-Decrease –Good soil/terrain	8059	448	0	33021	95614	52538	35078	*224758*
Dry-Neutral/Negative-Decrease -Bad soil/terrain	2299	61	61	48896	81022	55745	49283	*237366*
Dry-Neutral/Negative-Decrease -Unsuitable soil/terrain	702	61	61	27261	18307	29185	18428	*94005*
Subhumid-Neutral/Negative-Decrease -Good soil/terrain	22591	4102	10684	186243	9862	51836	1912	*287230*
Subhumid-Neutral/Negative-Decrease-Bad soil/terrain	24261	15173	15803	224963	11580	51195	3328	*346302*
Subhumid-Neutral/Negative-Decrease-Unsuitable soil/terrain	13189	9595	10563	186364	2880	22784	17400	*262776*
Humid-Neutral/Negative-Decrease -Good soil/terrain	31484	18053	17085	59774	17787	10370	714	*155267*
Humid-Neutral-Decrease/Negative–Bad soil/terrain	54341	29633	32646	71487	10817	6655	762	*206341*
Humid-Neutral-Decrease/Negative-Unsuitable soil/terrain	90302	87168	37244	84797	5251	4804	6534	*316100*
*Total area within biomass declining zone**	*247227*	*164294*	*124146*	*922807*	*253120*	*285112*	*133439*	*2130145*
Total area within SSA	*3370310*	*676922*	*808316*	*5729725*	*5559684*	*3211836*	*2323648*	*21680441*

* Differences between the total area of each land cover in this table and Table 4 are due to the edge errors. The error of total area is about 14 pixels (64 km²/pixel). The error of "Others" category is about 8 pixels, and those of other categories are less than 3 pixels each.

.

6. Summary and Conclusions

The objective of this study was to identify areas of land degradation in sub-Saharan Africa as observed from space by tracking the greenness of the vegetation signal expressed as NDVI over time. This study has utilized a series of existing databases and, through successive comparison of these, draws conclusions related to recent degradation of land in sub-Saharan Africa. Vegetation decline based on mean annual NDVI was used as a proxy for land degradation. The datasets (based on 8×8 km^2 pixels) of weather and NDVI-derived vegetation dynamics were averaged annually from monthly observations over the last two decades of the 20th century. This is likely to have captured reduced agricultural productivity as well as loss in native vegetation cover. First, we divided sub-Saharan Africa in dry (mean annual precipitation MAP <800 mm.yr-1), sub-humid (800 mm.yr-1 <MAP<1300 mm.yr-1) and humid dry (MAP >1300 mm.yr-1) regions, yielding three zones of similar geographic extent. In a second step we identified the regions where the annual vegetation reacts significantly to changes in mean annual rainfall conditions. For those with positive correlation, vegetation dynamics are affected by climate change (or cycles) and these are not suitable to identify human induced degradation. This excluded less than 2% from further analysis. In those with negative correlations the land shows either declining biomass despite improving rainfall suggesting serious degradation, or improving biomass despite a decline in rainfall. The latter is most likely due to human actions such as aforestation or irrigation (e.g Northern Sudan). These areas were relatively small (95.000 out of the 2.18 million km^2).

Subsequently the slope and the significance of the vegetation index (NDVI) over time were considered. Areas not showing a decline or increase in this vegetation index (NDVI), either in absolute or in relative terms, were considered stable vegetation covers. Those that showed an increase in vegetation index were predominantly found in the pastoral zone below the 500 mm isohyets and revealed a "greening of the Sahel" in the period evaluated. This has also been reported elsewhere. This region largely coincides with the region where NDVI fluctuations were positively correlated with rainfall which was excluded from this analysis of human induced land degradation. Large areas in of SSA showed a positive NDVI trend not related to rainfall. One possible explanation would be the CO^2 and NOx fertilization due to increased levels in the atmosphere. The areas that show a consistent and significant decline in NDVI (or land degradation) over time amounts to around 2.13 million km^2 or 10% of the SSA land mass. The characteristics of this area were analyzed in more detail.

Over 60 million people live on land that is losing its ability to produce green biomass presumably due to human activity. For each rainfall zone, the mean population densities in areas with declining vegetation were more or less the same as for the rainfall zone as a whole. However, the large majority of the declining areas is thinly populated, irrespective of the rainfall zone. This would suggest that these are marginal areas with limited bearing capacities to start with. The GLASOD study found for sub-Saharan Africa that land degradation at the time was more or less linearly correlated with population density. The conclusion from this study is more nuanced. Most of the land that is degrading is doing so with below average population densities. These regions are likely to get worse or will spread further as population continues to increase in most of sub-Saharan Africa. Donors should carefully analyze the sustainability of continued agricultural land use before embarking on measures or investments in agriculture to alleviate poverty in these regions. Some of these lands may be best taken out of cultivation. However, this study also identifies some degrading areas with high population densities. Often these are regions with high productive potential and in urgent need of remediation. It is here that fertilizer schemes and land conservation measures should be targeted as they are likely to be economically feasible.

A dataset derived from the FAO was used to delineate areas with different topographical and soil constraints. These datasets were overlaid on the map with the declining vegetations. For the terrain constraints, slopes over 25% and areas over 3500 m a.s.l. were considered unsuitable. Similarly, soil constraint classes 5 through 8 in the FAO classification were considered inappropriate for agriculture. The former covers less than 10.6 thousand km^2 and is negligible, but the latter cover nearly 0.67 million km^2 of the degrading area. Most likely farmers are occupying such marginal land due to land scarcity. Once denuded, such land is often not productive and exposed to the elements, causing water or wind erosion. Farmers seeking new land that move into such areas may do more harm to the environment than they do themselves good. The donor community should seek ways for these farmers to avoid occupying such land as remediation is difficult and costly. Nearly half of the remaining degrading land is on soils that are of rather poor quality. These soils may not easily be ameliorated and might never gain the resilience that good farm land requires.

In order to obtain a better insight into where exactly this degradation is occurring, the emerging land degradation map was cross referenced with the land use/land cover map of GLC2000. This allows differentiation of the degradation areas according to land use type. Of the 0.67 million km^2 that are not suitable for agriculture, 105 thousand km^2 are actually being farmed and probably should not be. Means should be found to offer alternatives to these farmers so that land can be restored over time. Of the 1.46 million km2 that are degrading but suitable for cultivation, 0.3 million km2 are actually farmed (agriculture and forest/cropland) and are likely over-exploited or poorly managed. Moreover, half of these are on poor soils and it may be too costly to restore such land. These are areas where considerable research efforts should be made to identify the immediate and proximate causes and develop more sustainable farming practises. A quarter million km^2 is under grassland, largely in the dry areas and most likely is being over-grazed. Nearly 1.09 million km^2 are under woodland/shrubland and forest/savanna, which each might be losing native trees as land

The fraction of the land showing significant decline in vegetation cover is relatively modest (around 10%). This would correspond with the fraction of SSA with "very severe" land degradation symptoms in the GLASOD assessment of late eighties. However, it is unlikely that any direct comparison between these two studies can in fact be made. It is more likely that these areas are additive, as the very severely degraded land from the GLASOD study would not likely show great further vegetation decline. The creeping additional loss of 10% over the last 20 years of the past century, if the pace is not slowed, translates into serious trouble for sub-Saharan Africa in the course of the current century.

It may be reasonable to assume that, when land degradation can be observed from space through declining biomass production, particularly on agricultural land, the underlying degradation processes must indeed be rather severe. Even though the extent of degradation from this assessment appears modest, much more degradation is likely to be on-going without being detectable (yet) with satellites. Moreover, land degradation on agricultural land seems to be taking place in the most productive areas of sub-Saharan Africa, threatening food production in the long run. Finally, this land degradation is happening against a background of increasing population and deteriorating climate conditions in a food insecure part of the world.

This assessment can only be seen as a first approximation, and the maps and assessments made here need further verification in the field. The analysis, in essence, is as good as the underlying databases. However, as better data becomes available the analysis framework proposed here allows for easy substitution of this information and rapid generation of a new assessment. As it stands, the following conclusions can be drawn that affect the research community:

- In the absence of any instruments for monitoring the rate of land degradation on the ground in SSA, satellite-based systems offer the best hope for tracking the state of this vital natural resource on this vast continent. A systematic research effort should be made to verify the validity of the findings reported here and to refine the analytical tool and interpretation of the results. As more and better data-bases are placed in the public domain the current study should be updated periodically.
- The current mapping exercise should be used to identify application domains, areas with common climatic, vegetation, physiographic and soil and land use characteristics that appear to be threatened by human induced land degradation. Based on this stratification, research organizations should be able to select pilot research sites where in-depth research can be undertaken to assess the total cost of land degradation (including the valuation of loss of ecosystem services) and design sustainable land management options that will maximize social benefits from the use of the land.
- Research should be undertaken to study the institutional arrangements around land access and tenure within the application domains in order to find means that will allow sustainable land management systems to be established equitably. In some cases this will be possible only through payment for ecosystem services (PES) for which the level and beneficiaries need to be determined. The use of such instruments should be an integral part of the strategy to preserve the land for future generations.

However, some of the regions identified in this study deserve immediate attention from the donor community and policy makers:

- Identify those agricultural regions where soil and terrain conditions seem so unfavourable that immediate action is required to restore the land to its natural condition. Donor agencies could offer incentives that lead to vacating such lands by offering alternative pathways out of poverty.
- Identify areas in the humid tropics where population pressures are low but NDVI change is high as such areas are likely being deforested. Where this is taking place on poor or unsuitable soil or terrain, these practices lead to denudation and should be stopped as the land is of little agricultural use and restoration of such land is a very slow process.
- Identify areas of favourable soil and terrain where population pressure is high and degradation is in full progress. These likely are relatively resilient regions that have served as breadbaskets of Africa and require immediate attention from the development community. These are areas where fertilizer markets and land conservation measures could function and are likely to be profitable.

It is likely that further conclusions can be derived from this analysis, but such would require a modicum of ground-truthing of the findings presented here. A more detailed insight of what land degradation is happening and where may be obtained through the web-based version of this study (www.zef.de) which includes a zoom function. This allows zeroing-in on countries or parts of countries. It provides access to the respective data-bases that were employed in this study so they can be called upon for further analysis by interested parties. In a further step, it is planned to allow local experts to upload verification data and degradation details so that, over time, a monitoring tool will be created to keep track of the land in sub-Saharan Africa, on which the development of the sub-continent ultimately depends.

References

Achard, F., Eva, H. and Mayaux, P. 2001. Tropical forest mapping from coarse spatial resolution satellite data: production and accuracy assessment issues. *International Journal of Remote Sensing* 22: 2741–2762.

Anyamba, A. and Tucker, C.J. 2005. Analysis of Sahelian vegetation dynamics using NOAA-AVHRR NDVI data from 1981–2003. *Journal of Arid Environments* 63: 596–614.

Bai, Z.G. and Dent, D.L. 2006. *Global Assessment of Land Degradation and Improvement: pilot study in Kenya.* Report 2006/01, World Soil Information (ISRIC), Wageningen, The Netherlands.

Bai, Z.G. and Dent, D.L. 2007. *Global Assessment of Land Degradation and Improvement: pilot study in South Africa.* Report 2007/01, World Soil Information (ISRIC), Wageningen, The Netherlands.

Bartalev, S., Belward, AS., Erchov, D. and Isaev, AS. 2003. A new SPOT4-VEGETATION derived land cover map of Northern Eurasia. *International Journal of Remote Sensing* 24: 1977–1982.

Beck, C., Grieser, J. and Rudolf, B. 2005. A new monthly precipitation climatology for the global land areas for the period 1951 to 2000. *Klimastatusbericht KSB 2004, DWD*: 181-190.

Billings, S.A., Zitzer, S.F., Weatherly, H., Schaeffer, S.M., Charlet, T., Arnone III, J.A. and Evans, R.D. 2003. Effects of elevated carbon dioxide on green leaf tissue and leaf litter quality in an intact Mojave Desert ecosystem. *Global Change Biology* 9: 729-735.

CIESIN/CIAT 2004. *Gridded population of the world, version 3*. Center for International Earth Science Information Network (CIESIN) and Centro Internacional de Agricultura Tropical (CIAT), Columbia University, NY, USA. (http://sedac.ciesin.columbia.edu/gpw/index.jsp).

Cihlar, J., Latifovic, R., Beaubien, J., Guindon, B. and Palmer, M. 2003. Thematic Mapper (TM) based accuracy assessment of a land cover product for Canada derived from SPOT VEGETATION (VGT) data. *Canadian Journal of Remote Sensing* 29: 154–170.

Dentener, F.J. 2006. Global maps of atmosphereic nitrogen deposition, 1860, 1993 and 2050. Data set. Available on-line (http://daac.ornl.gov/) from Oak Ridge National Laboratory Distributed Active Archive Center, Oak Ridge, Tennessee, U.S.A.

Dregne, H.E. and Chou, N.T. 1993. Global desertification dimensions. In: Dregne, H.E. (ed.) *Degradation and restoration of arid lands*. International Center for Arid and Semiarid Studies, Texas Tech University, Lubbock, Texas, USA, pp. 249-282.

Eastman, J.R. and Fulk, M. 1993. Long sequence time series evaluation using standardized principal components. *Photogrammetric Engineering and Remote Sensing* 59: 991–996.

Eklundh, L. and Olsson, L. 2003. Vegetation index trends for the African Sahel 1982–1999. Geophysical Research Letters 30(8), 1430, doi:10.1029/2002GL016772.

FAO 2007. Independent External Evaluation Report of the FAO. FAO, Rome Italy

FAO. 2000. *Land resources potential and constraints at regional and country level*. World Soil Resources Report No. 90. Rome, Italy.

Field, C.B., Randerson, J.T. and Malmström, C.M. 1995. Global net primary production: combining ecology and remote sensing. *Remote Sensing of the Environments* 51: 74-88.

Fischer, G., van Velthuizen, H., Shah, M. and Nachtergaele, F.O. 2002. *Global agro-ecological assessment for agriculture in the 21st century: methodology and results*. RR-02-02, FAO and IIASA, Laxenburg, Austria.

Fritz, S., Bartholome, E., Belward, A., Hartley, A., Stibig, H.-J., Eva, E., Mayaux, P., Bartalev, S., Latifovic, R., Kolmert, S., Roy, PS., Agrawal, S., Wu, B., Xu, W., Ledwith, M., Peckel, J.-F., Giri, C., Cher, MS., De Badts, E., Tateischi, R., Champeaux, J.-L. and Defourn, YP. 2003. *Harmonisation, mosaicing and production of the Global Land Cover 2000 database (Beta Version)*. Publication of the European Commission EUR 20849 EN. Office for Official Publications of the European Communities, Luxembourg.

GEF, 2006. *Global Environmental Facility: protecting the global environment – Africa*. (www.theGEF.org)

Giri, C., Zhu, Z. and Reed, B. 2005. A comparative analysis of the Global Land Cover 2000 and MODIS land cover data sets. *Remote Sensing of Environment*s 94(1): 123-132.

Greenland, D.J., Bowen, G., Eswaran, H., Rhodes, R., Valentin, C. 1994. Soil, water, and nutrient management research: a new agenda. IBSRAM Position Paper. IBSRAM, Bangkok, Thailand.

Groten, S.M.E. and Ocatre, R. 2002. Monitoring the length of the growing season with NOAA. *International Journal of Remote Sensing* 23(14): 1271-1318.

Herrmann, S.M., Anyamba, A. and Tucker, C.J. 2005. Recent trends in vegetation dynamics in the African Sahel and their relationship to climate. *Global Environmental Change* 15: 394–404.

Huxman, T.E., Smith, M.D., Fay, P.A., Knapp, A.K., Shaw, M.A., Loik, M.E., Smith, S.D., Tissue, D.T., Zak, J.C, Weltzin, J.F., Pockman, W.T., Sala, O.E., Haddad, B.M., Harte, J., Koch, G.W., Schwinning, S., Small, E.E. and Williams, D.G. 2004. Convergence across biomes to a common rain-use efficiency. *Nature* 429: 651-654

Ichii, K., Matsui Y., Murakami K., Yamaguchi Y., Ogawa K. 2002. Future projections of global environment due to anthropogenic CO^2 emission: analysis from a simplified carbon cycle model and climate coupled model and earth observation satellite data. *Journal of the Remote Sensing Society of Japan* (in Japanese with English abstract), 22(5): 625-636.

Kaizzi, C.K., H. Ssali and P.L.G. Vlek. 2006. Differential use and benefits of Velvet bean (Mucuna pruriens var. utilis) and N fertilizers in maize production in contrasting agro-ecological zones of E. Uganda. Agric. Systems: 88: 44-60.

Katyal, J.C. and Vlek, P.L.G. 2000. *Desertification - concept, causes and amelioration*. ZEF Discussion Paper 33. Center for Development Research, Bonn, Germany.

Knapp, A.K. and Smith, M.D. 2001. Variation among biomes in temporal dynamics of aboveground primary production. *Science* 291: 481-484.

Kottek, M., Grieser, J., Beck, C., Rudolf, B. and Rubel, F. 2006. World map of the Köppen-Geiger climate classification updated. *Meteorol. Zeitschr*. 15(3): 259–263.

Lepers, E. 2003. *Synthesis on the main areas of land-cover and land-use change*. Final report. September 2003. LUCC International Project Office.

Lovelock, J. 2006. *The revenge of Gaia*. Allen Lane, Pinguin Group. London, England.

Mayaux, P., Bartholome, E., Frtiz, S. and Belward, A. 2004. A new land-cover map of Africa for the year 2000. *Journal of Biogeography* 31: 861-877.

Mitchell, T.D. and Jones, P.D. 2005. An improved method for constructing a database of monthly climate observations and associated high-resolution grids. *International Journal of Climatology* 25: 693-712.

Moyo, S. 2000. *Land reform under structural adjustment in Zimbabwe: land use change in Mashonaland provinces*. Nordiska Afrika Institutet, Uppsala, Sweden.

Nicholson, S.E. Davenport, M.L. and Malo, A.R. 1990. A comparison of the vegetation response to rainfall in the Sahel and East Africa, using Normalized Difference Vegetation Index from NOAA AVHRR. *Climatic Change* 17: 209-241.

Norby, R.J. 1987. Nodulation and nitrogenase activity in nitrogen fixing woody plants stimulated by CO_2 enrichment of the atmosphere. *Physiologia Plantarum* 71: 77-82.

Oldemann, L.R., Hakkeling, R.T.A. and Sombrock, W.G. 1990. *World map of the status of human induced soil degradation: an explanatory note*. International Soil Reference and Information Center, Wageningen, The Netherlands.

Olsson, L. 1993. On the causes of famine: drought, desertification and market failure in the Sudan. *Ambio* 22: 395-403.

Olsson, L., Eklundh, L. and Ardö, J. 2005. A recent greening of the Sahel: trends, patterns and potential causes. *J. Arid Environ.* 63: 556-566.

Potter, C.S. and Brooks, V. 1998. Global analysis of empirical relationships between annual climate and seasonality of NDVI. *Int J Remote Sens.* 19: 2921–48.

Prince, S.D. and Goward, S.N. 1995. Global primary production: a remote sensing approach. *Journal of Biogeography* 22 (4/5): 815-835.

Prince, S.D., Brown, M.E., Colstoun, E. and Kravitz, L.L. 1998. Evidence from rain-use efficiency does not indicate extensive Sahelian desertification. *Global Change Biology* 4: 359–379.

Reich, R., Eswaren., H., Kapur, S. and Akca, E. 2001. *Land degradation and desertification in desert margins*. USDA Natural Resources Conservation Service.

Reynolds, J.F. and Smith, D.M.S. 2002. *Global desertification – do humans cause deserts*? Dahlem Workshop Report 88, Dahlem University Press, Berlin, Germany.

Sheng, T.C. 1990. *Watershed management field manual: watershed survey and planning*. FAO Conservation Guide 13/6. FAO, Rome, Italy.

Siebert, S. Döll, P., Hoogeveen, J., Faures, J.M., Frenken, K., and Feick, S. 2005. Development and validation of the global map of irrigation areas. *Hydrology and Earth System Sciences* 9: 535–547.

Siebert, S., Döll, P. and Hoogeveen, J. 2002. *Global map of irrigated areas version 2.1*. Center for Environmental Systems Research, University of Kassel, Germany, and FAO, Rome, Italy.

SSSA. 1996. *Glossary of Soil Science Terms*. Soil Science Society of America, Madison, Wisconsin, USA.

Stoorvogel, J.J. and Smaling, E.M.A. 1990. *Assessment of soil nutrient depletion in Sub-Saharan Africa: 1983-2000*. Report 28, the Winand Staring Centre for Integrated Land, Soil and Water Research, Wageningen, The Netherlands.

Syers, J.K., Lingard, J., Pieri, C. Ezcurra, E. and Faure, G. 1996. Sustainable land management for the semiarid and sub-humid tropics. *Ambio* 25: 484-491.

Tamene, L., S.J. Park, R. Dikau and P.L.G. Vlek. 2006. Analysis of factors determining sediment yield variability in the highlands of northern Ethiopia. Geomorphology 76: 76-91.

Tateishi, R. 2002. *Global Land Cover Ground Truth (GLCGT): Database version 1.2 (CD ROM).* (http://www.cr.chiba-u.jp/tateishi/publications.htm)

Temperton, V.M., Grayston, S.J., Jackson, G., Barton, C.V.M., Millard, P. and Jarvis, P.G. 2003. Effects of elevated carbon dioxide concentration on growth and nitrogen fixation in *Alnus glutinosa* in a long-term field experiment. *Tree Physiology* 23: 1051-1059.

Tissue, D.T., Thomas, R.B. and Strain, B.R. 1997. Atmospheric CO^2 enrichment increases growth and photosynthesis of *Pinus taeda*: a 4-year experiment in the field. *Plant, Cell and Environment* 20: 1123-1134.

Tucker, C.J. and Choudhury, B.J. 1987. Satellite remote sensing of drought conditions. *Remote Sensing of Environment* 23:243-252.

Tucker, C.J. and Nicholson, S.E. 1999. Variations in the size of the Sahara Desert from 1980 to 1997. *Ambio* 28: 587-591.

Tucker, C.J., Pinzon, J.E., Brown, M.E., Slayback, D.A., Pak, E.W., Mahoney, R., Vremote, E.F., El Saleous, N. 2005. An extended AVHRR 8-km NDVI data set compatible with MODIS and SPOT Vegetation NDVI data. *International Journal of Remote Sensing* 26(20): 4485-4498

UNEP. 1991. *Status of desertification and implementation of the United Nations Plan of Action to Combat Desertification*. Report of the Executive Director. UNEP/GCSS.III/3. Nairobi.

UNEP. 1992. *World Atlas of Desertification*. Edward Arnold, Sevenoaks, UK.

UNEP. 2002. Africa environment outlook: past, present and future perspectives. UNEP/ GRID-Arendal, Longum Park, Norway.

United Nations. 1994. *Earth Summit - Convention on Desertification*. Proceedings of the United Nations Conference on Environment and Development (UNCED), Rio De Janeiro, Brazil, 3-14 June 1992. Department of Public Information, United Nations, New York.

USGS. 2004. *Shuttle Radar Topography Mission, 30 Arc Second Resolution*. Global Land Cover Facility, University of Maryland, College Park, Maryland, February 2000. (http://glcf.umiacs.umd.edu/data/srtm/)

Van Lynden, G.W.J. and Kuhlmann, T. 2002. *Review of degradation assessment methods*. World Soil Information (ISRIC), Wageningen, The Netherlands.

Vlek, P.L.G. 2005. Nothing begets Nothing. The creeping disaster of land degradation. InterSecTions No 1. pp 28. United Nations University Institute for Environment and Human Security, Bonn Germany

Appendix 1
Pre-processing time-series AVHRR-NDVI data of African continent (1982 – 2003)

1. Data source:

The normalized differenced vegetation index (NDVI) product for a period of 22 year spanning from 1982 to 2003 was retrieved from the Global Inventory Modeling and Mapping Studies (GIMMS), published by the Global Land Cover Facility (GLCF) (http://glcf.umiacs.umd.edu/data/gimms/). The data set is derived from imagery obtained from the Advanced Very High Resolution Radiometer (AVHRR) instrument onboard the NOAA satellite series 7, 9, 11, 14, and 16. This is an NDVI dataset that has been corrected for calibration, view geometry, volcanic aerosols, and other effects not related to vegetation change. The GIMMS's data are downloadable via the FPT links: ftp://ftp.glcf.umiacs.umd.edu/glcf/GIMMS/Regional/Albers/Africa/. The downloaded data are signed 16-bit integer files, TIF format in Albers Equal Area Projection.

2. Processing steps:

1) Regional masking and boundary clipping:

We used ERDAS IMAGINE 8.3 to convert the TIF files (16-bit integer) to IMG files, then converted the Albers Equal Area Projection to Geographic Projection (Long/Lat WGS 1984).

The spatial coverage of downloaded data still covers a part of the Middle East. This non-African part was first masked, and then eliminated from the dataset.

2) Pixel-based masking and fixing errors:

We conducted pixel-based masking and fixing of errors for original NDVI values according to the GIMMS guide (http://glcf.umiacs.umd.edu/data/guide/technical/GIMMSdocumentation_NDVIg_8km_rev4.pdf, pp. 8-9). The signed 16-bit integer files above are referred to as the "raw" data.

In the "raw" data, pixels with a value of -10000 were converted to -0.1 (water), and pixels with a value of -5000 were masked (null data). Raw pixels of -2000 are considered as missing data, thus also masked as null areas.

To evaluate the quality of the raw data, FLAG value of a pixel was calculated as: FLAG = raw - floor(raw/10)*10. The meaning of the FLAG index is as follows: FLAG = 6 (missing data), FLAG = 5 (NDVI retrieved from average seasonal profile, possibly snow), FLAG = 4 (NDVI retrieved from average seasonal profile), FLAG = 3 (NDVI retrieved from spline interpolation, possibly snow), FLAG = 2 (NDVI retrieved from spline interpolation), FLAG = 1 (good value, possibly snow), FLAG = 0 (good value). Hence, pixels with FLAG > 1 were also masked as null data.

Lastly, we convert all remaining "raw" data to the standard NDVI (ranging from -1 to 1) using the following formula: NDVI = fix (raw/10000)

3. Description of final products:

1) Meta data:
   Geographic projection (long/lat)
   Datum: WGS 1984
   Grid header:

ncols	953
nrows	997
xllcorner	-17.676018
yllcorner	-35.004546
cellsize	0.072727272727273 (geographic degree, or equal to 8 km)
NODATA_value	-9999

2) Temporal resolution: monthly (average of two archives a month)

3) Exported format: standard ArcInfo ASCII file (*.asc)

Appendix 2
Pixel-based test of hypothesis concerning correlation coefficient

1. Theory

The correlation between X and Y can be measured by the Pearson's coefficient R_{xy}

$$R_{xy} = \frac{\sum (X_i - \overline{\overline{X}})(Y_i - \overline{Y})}{\sqrt{\sum (X_i - \overline{X})^2 \sum (Y_i - \overline{Y})^2}}$$

Suppose we want to test the hypothesis that the correlation of X and Y (R_{xy}) is zero:

$$H_0: R_{xy} = 0$$

We can use Fisher's transformation from R_{xy} to Z value that obeys normal distribution:

$$Z = \frac{1}{2} \ln\left(\frac{1 + R_{xy}}{1 - R_{xy}}\right)$$

The standard error of Z can be approximated to:

$$SE(Z) = \frac{1}{\sqrt{n-3}}$$

It follows that the test of hypothesis H_0 is the ratio

$$t_0 = Z / SE(Z)$$

which has a t-distribution with $df = n$-2. Suppose $t_{\alpha,df}$ is the theoretical ration (obeying t-distribution) at a confident level 1-α and the degree of freedom df, we can reject or accept hypothesis H_0 by comparing t_0 and $t_{\alpha,df}$:

- If $|t_0| \geq t_{\alpha,df}$: hypothesis H_0 is rejected. This means the correlation coefficient is significantly different from zero.
- If $|t_0| < t_{\alpha,df}$: hypothesis H_0 is accepted. This means the correlation coefficient is not significantly different from zero.

2. Pixel-based application for inter-annual NDVI and rainfall data:

Let: X_i is the mean annual precipitation (MAP), i = 1982 to 2002
Y_i is mean annual NDVI, i = 1982 to 2002
df = 21- 2 = 19

For each pixel:

- Calculating Z, $SE(Z)$ and the ratio $t_0 = Z / SE(Z)$
- If $|t_0| \geq t_{0.25,19} = 0.687$ then the calculated R_{xy} is significantly different from zero at the confident level of 75%.
- If $|t_0| \geq t_{0.1,19} = 1.328$ than the calculated R_{xy} is significantly different from zero at the confident level of 90%.
- If $|t_0| \geq t_{0.05,19} = 1.729$ then the calculated R_{xy} is significantly different from zero at the confident level of 95%.

This computation was done using matrix algebra in Spatial Analyst module (an extension of ArcView GIS 3.2).

Appendix 3
Pixel-based test of hypothesis concerning slope coefficient in simple linear repression

1. Theory

Assuming *X* and *Y* have a stochastically linear relationship:

$$Y = AX + B + \varepsilon$$

where: *A*- slope *B*- intercept ε – random error/disturbance

We thus define:

$$S_{xx} = \sum (X_i - \overline{X})^2$$
$$S_{yy} = \sum (Y_i - \overline{Y})^2$$
$$S_{xy} = \sum (X_i - \overline{X})(Y_i - \overline{Y})$$

Hence, the least square estimator for slope *A* and intercept *B* are:

slope: $A_{cal} = \dfrac{S_{xy}}{S_{xx}}$ and intercept $B = \overline{Y} - A_{cal}\overline{X}$

The coefficient of determination is given by:

$$R^2 = \frac{S_{xy}^2}{S_{xx}S_{yy}}$$

The residual sum of squares is given by:

$$RSS = S_{yy}(1 - R^2)$$

Suppose we want to test the hypothesis that the true value of *A* is zero:

$$\boldsymbol{H_0: A = 0}$$

It follows that the test for significant of *A* is the ratio:

$$t_0 = \frac{A_{cal}}{SE(a)}$$

where *SE*(*A*) is the standard error of the slope coefficient:

$$SE(A) = \sqrt{Var(A)} = \sqrt{Var(\varepsilon)/S_{xx}}$$

The variance of error $Var(\varepsilon)$ can be unbiasedly estimated by:

$$Var(\varepsilon) = \frac{RSS}{n-2} = \frac{S_{yy} - A_{cal}S_{xy}}{n-2}$$

Thus, we have: $SE(A) = \sqrt{Var(\varepsilon)/S_{xx}} = \sqrt{\dfrac{S_{yy} - A_{cal}S_{xy}}{(n-2)S_{xx}}}$

Suppose $t_{\alpha,df}$ is the theoretical ratio (obeying t-distribution) at a confidence level 1-α and a degree of freedom *df* (known from *t*-table), we can reject or accept the hypothesis H_0 by comparing t_0 and $t_{\alpha,df}$:

- If $|t_0| \geq t_{\alpha,df}$: The hypothesis H_0 is rejected. This means the calculated slope coefficient is significantly different from zero.
- If $|t_0| < t_{\alpha,df}$: The hypothesis H_0 is accepted. This means the calculated slope coefficient is not significantly different from zero.

2. Pixel-based application for inter-annual NDVI data:

Let: X_i is considered year, i = 1982 to 2003
Y_i is mean annual NDVI, i = 1982 to 2003
df = 22-2 = 20

For each pixel:

- Calculating A_{cal}, $SE(A)$ and the ratio $t_0 = Z / SE(Z)$
- If $|t_0| \geq t_{0.25,20} = 0.687$ then the calculated A_{cal} is significantly different from zero at the confident level of 75%.
- If $|t_0| \geq t_{0.1,20} = 1.325$) then the calculated A_{cal} is significantly different from zero at the confident level of 90%.
- If $|t_0| \geq t_{0.05,20} = 1.725$ then the calculated A_{cal} is significantly different from zero at the confident level of 95%.

This computation was done using matrix algebra in Spatial Analyst module (an extension of ArcView GIS 3.2).

Appendix 4
Sources of data used for the study

Data	*Hosting organization*	*Downloadable link*
NOAA-AVHRR NDVI (GIMMS) (8km × 8km)	Global Land Cover Facility (GLCF) at the University of Maryland (http://glcf.umiacs.umd.edu/data/gimms/)	ftp://ftp.glcf.umiacs.umd.edu/glcf/GIMMS/Regional/Albers/Africa/
Gridded climate of the world CRU TS 2.1 (0.5° × 0.5°)	Climate Research Unit (CRU) at the University of East Anglia (http://www.cru.uea.ac.uk/)	http://www.cru.uea.ac.uk/cru/data/hrg/cru_ts_2.10/
Gridded population of the world, version 3 (GPWv3)	Center for International Earth Science Information Network (CIESIN) at Columbia University (http://www.ciesin.org/)	http://sedac.ciesin.columbia.edu/gpw/continent.jsp?region=Africa
Global land cover GLC2000 (1km × 1km)	Global Vegetation Monitoring (GVM) Unit of the European Commission's Joint Research Centre (JRC) (http://www-gvm.jrc.it/glc2000/)	http://www-gvm.jrc.it/glc2000/ProductGLC2000.htm
Global digital elevation SRTM (1km × 1km)	Global Land Cover Facility (GLCF) at the University of Maryland (http://glcf.umiacs.umd.edu/data/srtm/)	ftp://ftp.glcf.umiacs.umd.edu/glcf/SRTM/GTOPO/
Soil constraints from Global Agro-ecological Assessment for Agriculture by IIASA-FAO (0.5° × 0.5°, or 5 arc-minute × 5 arc-minute)	The International Institute for Applied Systems Analysis (IIASA) and the Food and Agriculture Organization (FAO) of the United Nations (http://www.iiasa.ac.at/Research/LUC/SAEZ/index.html)	Soil depth constraints: http://www.iiasa.ac.at/Research/LUC/SAEZ/plates/zip/plate21.zip Soil fertility constraints: http://www.iiasa.ac.at/Research/LUC/SAEZ/plates/zip/plate22.zip Soil drainage constraints: http://www.iiasa.ac.at/Research/LUC/SAEZ/plates/zip/plate23.zip Soil texture constraints: http://www.iiasa.ac.at/Research/LUC/SAEZ/plates/zip/plate24.zip Soil chemical constraints: http://www.iiasa.ac.at/Research/LUC/SAEZ/plates/zip/plate25.zip Soil constraints combined: http://www.iiasa.ac.at/Research/LUC/SAEZ/plates/zip/plate27.zip